

Metabolic Profiling of S-praziquantel: Structure Elucidation Using the Crystalline Sponge Method in Combination with Mass Spectrometry and Nuclear Magnetic Resonance[§]

Lara Rosenberger, Judith Jenniches, Carolina von Essen, Anupam Khutia, Clemens Kühn, Andreas Marx, Katrin Georgi, Anna K. H. Hirsch, Rolf W. Hartmann, and Lassina Badolo

Merck KGaA, Darmstadt, Germany (L.R., J.J., C.v.E., A.K., C.K., A.M., K.G., L.B.); Helmholtz-Institute for Pharmaceutical Research Saarland (HIPS) - Helmholtz Centre for Infection Research (HZI), Saarbrücken, Germany (L.R., A.K.H.H., R.W.H.); and Department of Pharmacy, Saarland University, Saarbrücken, Germany (L.R., A.K.H.H., R.W.H.)

Received September 2, 2021; accepted January 15, 2022

ABSTRACT

Praziquantel (PZQ) is the drug of choice for treatment of the neglected tropical disease schistosomiasis. Although the drug has been extensively used over several decades and its metabolism well studied (several oxidative metabolites are known from literature), the knowledge of the complete structure of some of its metabolites remains elusive. Conventional techniques, such as nuclear magnetic resonance or liquid chromatography mass spectrometry were used in the past to investigate phase I and phase II metabolites of PZQ. These techniques are either limited to provide the complete molecular structure (liquid chromatography mass spectrometry) or require large amount of sample material (NMR), which are not always available when *in vitro* systems are used for investigation of the metabolites. In this study, we describe new structures of S-PZQ metabolites generated *in vitro* from human liver microsomes using the crystalline sponge method. After chromatographic separation and purification of the oxidative metabolites, ultra-performance liquid chromatography-quadrupole time-of-flight mass spectrometry analysis was

conducted to narrow down the position of oxidation to a certain part of the molecule. To determine the exact position of hydroxylation, single-crystal X-ray diffraction analysis of the crystalline sponges and absorbed analyte was used to identify the structure of S-PZQ and its metabolites. The crystalline sponge method allowed for complete structure elucidation of the known metabolites S-*trans*-4'-hydroxy-PZQ (M1), S-*cis*-4'-hydroxy-PZQ (M2) and S-*R*-11b-hydroxy-PZQ (M6) as well as the unknown metabolites S-9-hydroxy-PZQ (M3) and S-7-hydroxy-S-PZQ (M4). For comparison of structural elucidation techniques, one metabolite (M3) was additionally analyzed using NMR.

SIGNIFICANCE STATEMENT

The information content of the metabolic pathway of praziquantel is still limited. The crystalline sponge method allowed the complete structural elucidation of three known and two unknown metabolites of S-praziquantel, using only trace amounts of analyte material, as demonstrated in this study.

Introduction

Schistosomiasis is a neglected tropical disease caused by a parasitic flatworm of the genus *Schistosoma* and affects almost 240 million people worldwide, with a high prevalence in Africa. The World Health Organization implemented a program for schistosomiasis control over the past 40 years and recommends the anthelmintic drug praziquantel (PZQ) as the treatment of choice for all forms of the disease (WHO, 2011, 2020). PZQ is currently used as a racemic formulation in therapy; however, the activity is mainly associated with the *R*-enantiomer (Meister et al., 2014; Kovač et al., 2017). Although the drug has been known and extensively used since the early 1980s, the information content of the metabolic pathway is limited. Enantioselective transformation of

R-PZQ and *S*-PZQ has been explored in various studies, showing different metabolic profiles for both enantiomers (Wang et al., 2014; Vendrell-Navarro et al., 2020; Park et al., 2021). Several mono-oxidized (+16 Da) and secondary oxidative metabolites (+32 and +14 Da) are known from the literature, but most of their complete structures are still unknown. The main metabolite in human is 4'-hydroxy-PZQ and the position of hydroxylation was identified both in *cis* and *trans* configuration (Nleya et al., 2019). Two more metabolites have been described as 8-hydroxy-PZQ and 11b-hydroxy-PZQ by isolation from human urine and *in vitro* recombinant human P450 reactions, using NMR for data analysis (Schepmann and Blaschke, 2001; Vendrell-Navarro et al., 2020). Additional metabolites have been analyzed using different liquid chromatography mass spectrometry (LC-MS) systems, giving information of the type of metabolism (*i.e.*, hydroxylation, dehydrogenation and glucuronidation) and allowing to narrow down the site of metabolism to a certain part of the molecule (Lerch and Blaschke, 1998; Huang et al., 2010; Wang et al., 2014). Despite the advantage of LC-MS techniques to reach high sensitivity for sample analysis from *in vitro* origin, these techniques failed to identify the complete structure of metabolites.

This work received no external funding.

The authors declare a conflict of interest. L.R., J.J., C.v.E., A.K., C.K., A.M., K.G. and L.B. are employees of Merck KGaA, Darmstadt, Germany.

dx.doi.org/10.1124/dmd.121.000663.

§ This article has supplemental material available at dmd.aspetjournals.org.

ABBREVIATIONS: CS, crystalline sponge; CS-XRD, crystalline sponge method; HLM, human liver microsome; HPLC, high-performance liquid chromatography; LC-MS, liquid chromatography-mass spectrometry; PZQ, praziquantel; qTOF, quadrupole time-of-flight mass spectrometry; R_1 , residual factor; R_{int} , internal R-value; tpt, 2,4,6-tris(4-pyridyl)-1,3,5-triazine; UPLC, ultra-performance liquid chromatography.

A new approach for structural elucidation of compounds was introduced in 2013 by Makoto Fujita and is commonly known as the “crystalline sponge method” (CS-XRD) (Inokuma et al., 2013). The method enables crystal structure determination without the limitation of crystallization with only nanogram to a few microgram of analyte material. A metal coordination complex $[(ZnX_2)_3(tp)_2]_n \cdot x(\text{solvent})_m$ ($X=I$; $tp=2,4,6$ -tris(4-pyridyl)-1,3,5-triazine) is used as a pre-existing crystal and functions as a host. During a “soaking process”, the analyte (guest) is absorbed into the pores of the three-dimensional framework via diffusion and regularly ordered by intermolecular, noncovalent interactions and thus accessible for X-ray diffraction analysis (Inokuma et al., 2016; Brunet et al., 2017; Sakurai et al., 2017). We recently demonstrated that CS-XRD is a valuable tool, which can be applied to identify the exact position of metabolism for phase I and phase II metabolites generated in low amounts from *in vitro* incubation (Rosenberger et al., 2020).

In this study, we apply the CS-XRD for the determination of the absolute structures of *S*-PZQ and six of its hydroxylated metabolites after incubation with human liver microsome (HLM).

Materials and Methods

Chemicals and Reagents. *S*-PZQ, *S*-*cis*-4'-hydroxy-PZQ and *S*-*trans*-4'-hydroxy-PZQ were obtained from Merck KGaA small molecule library. Dipotassium hydrogen phosphate, potassium dihydrogen phosphate, magnesium chloride hexahydrate, cyclohexane, *n*-hexane, dihydronicotinamide adenine dinucleotide phosphate tetrasodium salt, DMSO-*d*₆, water (ultra-high-performance LC-MS grade), and acetonitrile (ultra-high-performance LC-MS grade) were purchased from Merck KGaA (Darmstadt, Germany). Zinc iodide, 1,2-dimethoxyethane, and formic acid were purchased from Sigma Aldrich Chemie GmbH (Steinheim, Germany). Tpt was purchased from abcr GmbH (Karlsruhe, Germany). Mixed gender HLM (Ultrapol, pool of 150) were purchased from Corning (Corning, USA).

Metabolism of *S*-PZQ by HLM. The hydroxylation of *S*-PZQ was conducted with an incubation mixture containing 0.5 mg/ml of HLM, 50 mM of potassium phosphate buffer (pH 7.4), 1 mM of magnesium chloride, and 200 μM of substrate. After 5 minutes of preincubation (37°C, 150 rpm), the reaction was initiated by the addition of nicotinamide adenine dinucleotide phosphate (NADPH, 1.5 mM), and the mixture was incubated for another 24 hours (final volume: 5.40 ml). After 6 hours, the reaction was boosted by addition of NADPH (1.5 mM).

The reaction was quenched by adding one volume of ice-cold acetonitrile and the precipitated proteins were removed by centrifugation at 4000 g for 1 hour at 4°C. The supernatant was evaporated to dryness (nitrogen flow, 40°C) and resolubilized in acetonitrile/water (20:80). 100 μl aliquots were used for purification and fractionation by high-performance liquid chromatography coupled with mass spectrometry (HPLC-MS).

Ultra-Performance Liquid Chromatography-Quadrupole Time-of-Flight Mass Spectrometry. The supernatants were analyzed on a Waters Acquity ultra-performance liquid chromatography (UPLC) system combined with a Xevo G2-S qTOF (Waters Corporation). Analysis was performed with an electrospray ion source in positive ion mode. For MS scan, the quadrupole time-of-flight mass spectrometry (qTOF) was operating with a source temperature at 150°C, a desolvation temperature at 600°C and a capillary voltage at 0.5 kV. For full-scan MS mode, the collision energy was set to 4 V, and the mass range was set to *m/z* 100 to 1000. For MS/MS studies, qTOF MS^c acquisition was conducted using a collision energy ranging from 25 to 40 V.

Metabolite separation was achieved on a chiral Lux Cellulose-2 column (150-2 mm, 3 μm; Phenomenex) equipped with a Lux Cellulose-2 precolumn (3 mm inner diameter; Phenomenex) at a flow rate of 0.45 ml/min over a period of 20 minutes using solvent A (water + 0.1% formic acid) and solvent B (acetonitrile + 0.1% formic acid) as mobile phases. The column oven temperature was set to 40°C. Elution was performed using a gradient from 20 to 90% B in 15 minutes, 90 to 95% B in 0.2 minutes, 95% B for 2.1 minutes, returning to 20% B in 0.1 minutes and re-equilibration at 20% B for 2.6 minutes. The software UNIFI version 1.9.4 (Waters Corporation) was used

to support the identification of metabolites. The metabolites were evaluated for mass error (≤ 4 ppm), fragmentation pattern and retention time.

HPLC-MS. The supernatants were analyzed and fractionated on an Acquity Arc HPLC system (Waters Corporation). The equipment components were described in detail in our previous work (Rosenberger et al., 2020).

Samples were analyzed with electrospray ionization mass spectrometry in positive ionization mode within an acquisition range from *m/z* 100 to *m/z* 650 in continuum mode and a sampling frequency of 2 Hz. The capillary voltage and the cone voltage were set to 0.8 V and 10.0 V, respectively. The probe temperature was set to 600°C. The mass value of *m/z* 329 was registered by the MS detector and triggered the fractionation of the target analytes. The software MassLynx 4.2 and FractionLynx were used for data acquisition and sample fractionation.

HPLC separation for M4 and M6 PZQ was performed with two Chromolith Performance RP18e columns (100-4.6 mm; Merck KGaA) for primary chromatographic purification and one Purospher Star RP18e Hibar HR column (100-2.1 mm, 2 μm; Merck KGaA) as second chromatographic system. The column oven temperature was set to 25°C. For the first purification, elution was performed at a flow rate of 1.0 ml/min using solvent A (water) and solvent B (acetonitrile) as mobile phases. The analytes were eluted over a period of 30 minutes, using a multi-segmented gradient from 0% to 25% B in 7 minutes, 25% to 30% B in 3 minutes, 30% to 80% B in 10 minutes, 80% B for 5 minutes, returning to 0% B in 0.1 minutes, and re-equilibration at 0% B for 4.9 minutes. The eluent was directed to the waste during the first 5 minutes to reduce contamination. For the second purification, elution was performed at a flow rate of 0.45 ml/min over a period of 15 minutes, applying the following gradient: mobile phase 0% to 60% for 10 minute, 60% B to 100% B in 2 minute; 100% to 0% B in 0.1 minutes and re-equilibration at 0% B for 2.9 minutes.

HPLC separation for M3, M5, and additionally M6 PZQ was achieved using an additional third purification step. The further purification was performed using the Lux Cellulose-2 column and gradient described as before. Differences were the column oven temperature of 25°C and the solvent A (water) and solvent B (acetonitrile) as mobile phases.

Following each chromatographic separation step, the collected fractions were pooled, evaporated to dryness at 40°C under nitrogen flow and resolubilized in acetonitrile/water (20:80) for further purification. After final purification, the collected fractions from each metabolite were combined and evaporated to dryness to conduct the crystalline sponge (CS) soaking and NMR measurement.

CS-XRD. The porous CS $[(ZnI_2)_3(tp)_2]_n \cdot x(\text{cyclohexane})_m$ (**1a**) and $[(ZnI_2)_3(tp)_2]_n \cdot x(\text{n-hexane})_m$ (**1b**) were prepared according to the procedures known from literature (Biradha and Fujita, 2002; Ramadhar et al., 2015).

For guest soaking of *S*-PZQ, a single crystal of **1a** was transferred with 50 μl of cyclohexane to a glass vial. After addition of 2 μl of dissolved analyte solution (1 mg/ml in 1,2-dimethoxyethane), the sample vial was closed with a screw cap and the septum seal was pierced with a syringe needle, before placing it in an incubator at 50°C for 1 day. Following evaporation of solvent, the vial was placed without a needle for 2 days at 4°C to increase guest occupancy and hence the chirality transfer from the guest molecules to the CS framework. For *S*-*trans*-4'-hydroxy-PZQ, one crystal of **1b** was used and analyzed after evaporation of *n*-hexane after 1 day. The soaking condition for *S*-*cis*-4'-hydroxy-PZQ was adjusted by reducing the volume of *n*-hexane to 25 μl, the temperature for solvent evaporation to 25°C and the soaking time to 3 days by using a syringe needle with smaller diameter. Soaking of incubation samples (about 1–2 μg) was conducted similarly to the reference material. Two microliters of 1,2-dimethoxyethane, 50 μl of cyclohexane and one CS (**1a**) were pipetted into the vial, which contained the pooled metabolite material. The incubator temperature was set to 50°C and the evaporation time was one day.

Single-crystal X-ray diffraction measurements were performed by using a Rigaku Oxford Diffraction XtaLAB Synergy-R diffractometer (Cu-K_α, $\lambda = 1.54184 \text{ \AA}$) at a temperature of 100 K and crystal structure modeling using OLEX2 (Dolomanov et al., 2009), SHELXT, and SHELXL (Sheldrick, 2015) were conducted as described in detail in our previous work (Rosenberger et al., 2020). The software ShelXle was used to generate the electron density maps of *S*-PZQ and its hydroxy metabolites (Hübschle et al., 2011).

NMR of PZQ Metabolite M3. Structural elucidation of metabolite M3 was performed at 298 K using a 700 MHz Bruker Avance III equipped with a 5-mm cryocooled triple resonance probe. The isolated metabolite (about 15 μg) was dissolved in 200 μl of DMSO-*d*₆ and transferred into a 3 mm NMR tube.

The ^1H NMR spectrum was acquired with 64 k time domain points, a spectral width of 20 ppm, a relaxation delay of 10 seconds, and 1024 scans. Edited heteronuclear single quantum coherence NMR spectrum was recorded with 1024×256 time domain data points over a spectral width of 12 ppm in the t_2 and 165 ppm in the t_1 dimension. The homonuclear correlation spectroscopy NMR spectrum was acquired with 1024×256 time domain data points over a spectral width of 12 ppm in the t_2 and t_1 dimension. The rotating frame Overhauser enhancement effect spectroscopy NMR spectrum was recorded with 1024×256 time domain data points over a spectral width of 12 ppm in the t_2 and t_1 dimension. The software MestReNova version 14.1.0 (Mestrelab Research) was used for data analysis.

Results

UPLC-qTOF Analysis of S-PZQ Metabolites Prepared by Incubation with HLM. Both enantiomers of PZQ (Fig. 1) were incubated with HLM for 24 hour respectively, for metabolite profiling and identification (data not shown). S-PZQ showed an increased formation of metabolites and was therefore chosen for further analysis. During the study of metabolic stability, the UPLC-qTOF chromatogram of S-PZQ, incubated with HLM in the presence of NADPH, showed the formation of several oxidative metabolites (+16, +32 and +14 Da), which is in line with already published data (Huang et al., 2010; Wang et al., 2014). The incubation of S-PZQ without cofactor was conducted in parallel and showed no formation of metabolites, indicating their generation by enzymatic reaction. The analysis presented in this study, however, focuses on six monohydroxylated metabolites of S-PZQ (M1–M6).

The metabolites M1–M6 were detected at a protonated molecular mass $[\text{M}+\text{H}]^+$ of m/z 329. The increased m/z value of 16 Da, compared with the $[\text{M}+\text{H}]^+$ ion of the parent (m/z 313), suggested the addition of one oxygen to the molecular scaffold.

The mono-oxidized metabolites were further analyzed based on their MS/MS spectra and accurate mass measurements (Fig. 2, Supplemental Table 1). The mass spectrum ($[\text{M}+\text{H}]^+$) of M1 and M2 showed similar fragment ion peaks as the parent compound. The main fragment ions at m/z 203 and m/z 174 were assigned to the “core moiety” (*i.e.*, hexahydro-pyrazino [2,1-*a*]isoquinolin-4-one), indicating that the oxidation occurred at the cyclohexane ring. Metabolites M1 and M2 were identified as *S-trans*-4'-hydroxy-PZQ and *S-cis*-4'-hydroxy-PZQ by comparison of the respective retention time with the reference material.

The main fragment ions at m/z 219, m/z 190, m/z 162 and m/z 148, observed in the spectra of both M3 and M5, were assigned to an oxidized core moiety, indicating that the hydroxylation occurred somewhere at the tetrahydro-isoquinoline ring system. The full-scan mass spectrum of metabolites M4 and M6 showed the abundant ion m/z 311, representing a predominant loss of water ($329 \rightarrow 311$). In addition, both metabolites fragmented to form characteristic ions of m/z 201, m/z 144 and m/z 130, indicating a spontaneous water loss of the fragment ions observed for M3 and M5. The loss of water is predominantly

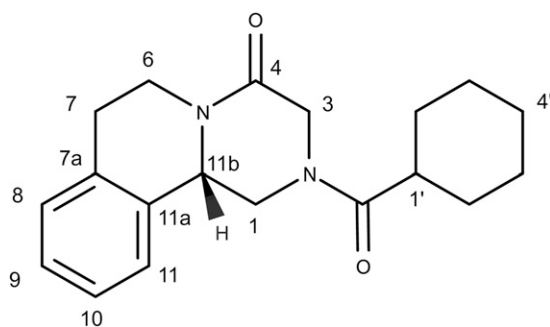


Fig. 1. Chemical structure of S-praziquantel.

observed for aliphatic hydroxylation, whereas it is less common for hydroxylation reactions, which occur on phenyl rings (Ramanathan et al., 2000; Holčápek et al., 2010). Therefore, it is likely that the addition of one oxygen occurred in the aliphatic part of the core moiety and not on the aromatic benzene.

The tandem mass spectrometry fragmentation pattern allowed to limit the oxidation to a certain part of the molecule but could not reveal the actual positions of hydroxylation. The metabolite structures of S-PZQ were therefore further analyzed using CS-XRD and NMR.

Structural Elucidation of S-PZQ Metabolites (M1–M4 and M6) by CS-XRD. For successful structure determination using CS-XRD, the optimization of soaking conditions (*e.g.*, CS type, solvent, temperature, time) is the crucial step. Thereby, various parameters need to be examined for every analyte (Hoshino et al., 2016). The optimal soaking parameters for S-PZQ were selected by conducting a CS affinity screening and examining the affinity of target analyte to CS framework using two CS types $[(\text{ZnI}_2)_3 \cdot (\text{tpt})_2]_n \cdot x(\text{solvent})_m$ and $[(\text{ZnCl}_2)_3 \cdot (\text{tpt})_2]_n \cdot x(\text{solvent})_m$; solvent=cyclohexane, *n*-hexane) at three different temperatures (50°C, 25°C, 4°C) (data not shown). The screening method has been described in detail in our previous work (Rosenberger et al., 2021). The optimal soaking conditions were then applied for S-PZQ and its mono-oxidized metabolites. To increase the occupancy of the analyte in the CS pores and to maximize the intermolecular interactions between CS framework and guest molecules, the soaking time was further adjusted for some analytes.

The parent active pharmaceutical ingredient and the reference metabolites *S-trans*-4'-hydroxy-PZQ (M1) and *S-cis*-4'-hydroxy-PZQ (M2) could successfully be structurally elucidated with CS-XRD using a conventional X-ray diffractometer. The crystal structure of S-PZQ revealed one guest molecule with an occupancy of 64% and one additional cyclohexane molecule with final residual factor (R_1) and internal R-factor (R_{int}) values of 8.23% and 3.08%, respectively. A Flack parameter of 0.234(8) was obtained, suggesting that the absolute configuration PZQ is *S*. One molecule of metabolite M1 was assigned by its electron density in the asymmetric unit with an occupancy of 52% (R_1 6.58% and R_{int} 3.86%, $\chi = 0.229(8)$). First analysis of the reference material M2 resulted in the determination of the hydroxy group at the 4'-cyclohexyl moiety in *trans* configuration. Pharmacokinetic data from previous studies showed the preferred formation of M1 and a *cis* to *trans* interconversion (Nleya et al., 2019; Vendrell-Navarro et al., 2020). To influence the less favored axial position of the substituent as little as possible, the soaking process was further optimized by decreasing the temperature to 25°C. As a result, one guest molecule in *cis* configuration could be assigned to M2 (occupancy 54%, R_1 5.85%, R_{int} 2.86%, $\chi = 0.328(8)$).

Next, CS-XRD was applied to the mono-hydroxylated metabolites of S-PZQ generated by *in vitro* incubation. The formation of several metabolites in different quantities was observed, necessitating an extensive chromatographic separation and purification process to fractionate the very closely eluting metabolites (Fig. 3A). To generate the sample amount in high purity, M4 and M6 were purified using two different chromatographic columns. M3 and M5 were thereby detected as one peak, requiring further separation using a third column (Fig. 3B). To estimate the amounts of M3–M6, the MS (for M3 and M5) and UV (for M4 and M6) signals of the reference material M2 were used. Thereby, an increase in the UV-VIS absorption maxima was observed for M3 (278 nm) and M5 (281 nm) compared with S-PZQ or M6 (263 nm), indicating an aromatic hydroxylation at the benzene moiety.

To reveal the exact position of hydroxylation, the soaking experiments were conducted under similar conditions as used for the parent compound to elucidate the structure of metabolites M3–M6. XRD measurements of the soaked CS allowed the crystallographic analysis of the metabolite structures. M6 shows high electron density at position 11b of

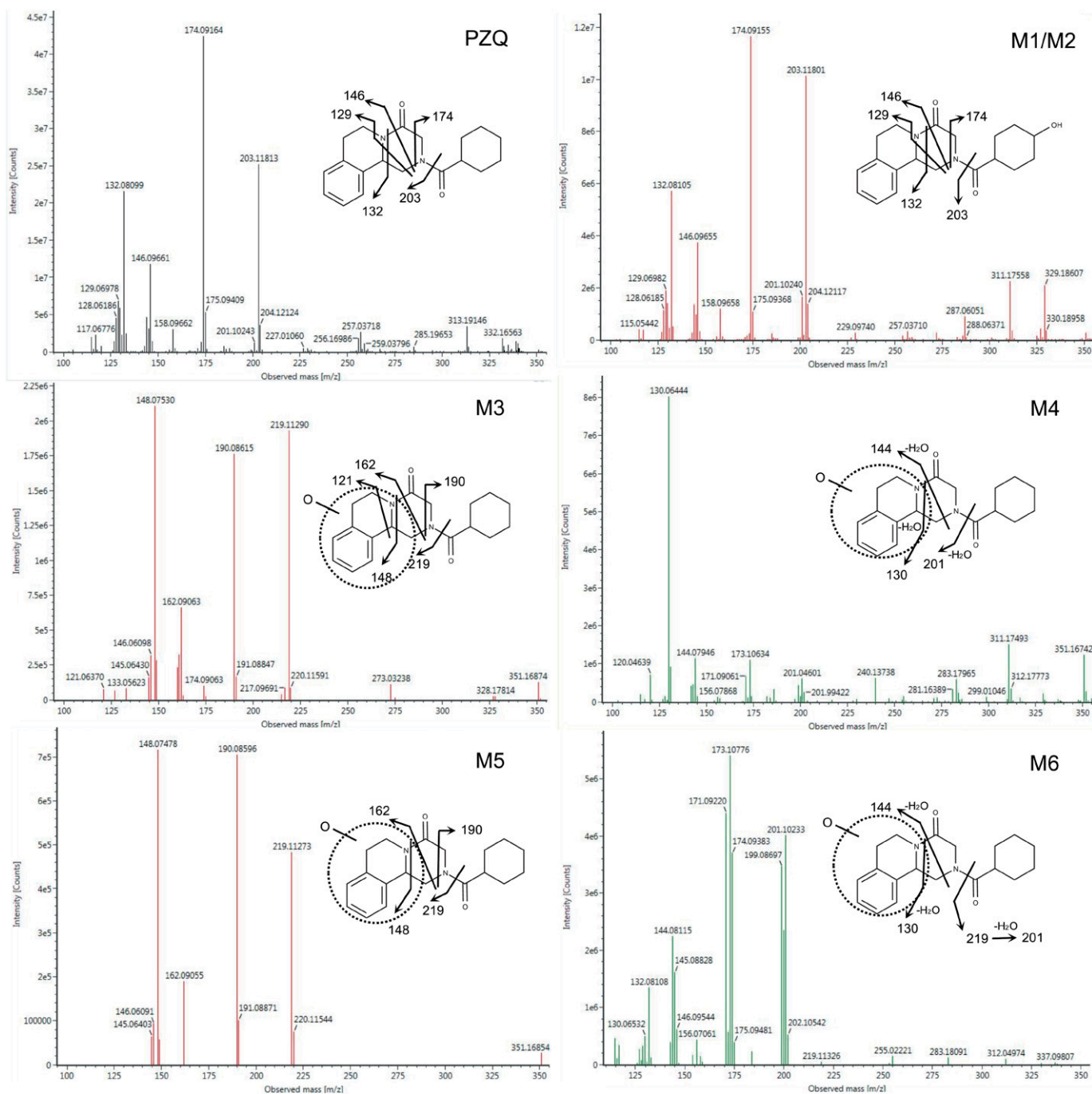


Fig. 2. Tandem mass spectrometry spectra and proposed structures of *S*-praziquantel and its metabolites M1–M6.

the isoquinoline ring system, confirming the structure elucidated via NMR in previous works (Vendrell-Navarro et al., 2020). High electron density in close proximity to the isoquinoline part was also observed for M4 at position 7 and M3 at position 9. Metabolite M5 shows diffuse electron density in the CS pores, but no structure could be successfully assigned. The electron density map of the “core moiety” from *S*-PZQ and its successfully elucidated metabolites are shown in Fig. 4.

Crystallographic data of M3 revealed one analyte molecule with an occupancy of 60% (R_1 5.53%, R_{int} 1.52%, $\chi = 0.204(7)$) and two cyclohexane molecules.

The crystal structure of M4 revealed one molecule with an occupancy of 76%, three cyclohexane molecules, and final R_1 and R_{int} values of

4.99% and 1.45%, respectively. The addition of one oxygen at position 7 of the molecule caused the creation of a second chiral center, which could be determined as *S* configuration indicated on the Flack parameter value of 0.191(7).

As already observed for the other metabolites and the parent compound, M6 was expected to be enantiopure. Surprisingly, an inconclusive Flack parameter of 0.5, indicating a racemic mixture, was observed. Furthermore, when analyzing the CS pores, both *S*- and *R*-11b-hydroxy-PZQ (occupancy 40% and 30%) were observed (R_1 5.92%; R_{int} 2.48%). The observation was further confirmed by chiral chromatography with the separation of both enantiomers. After chromatographic separation and purification, both enantiomers were

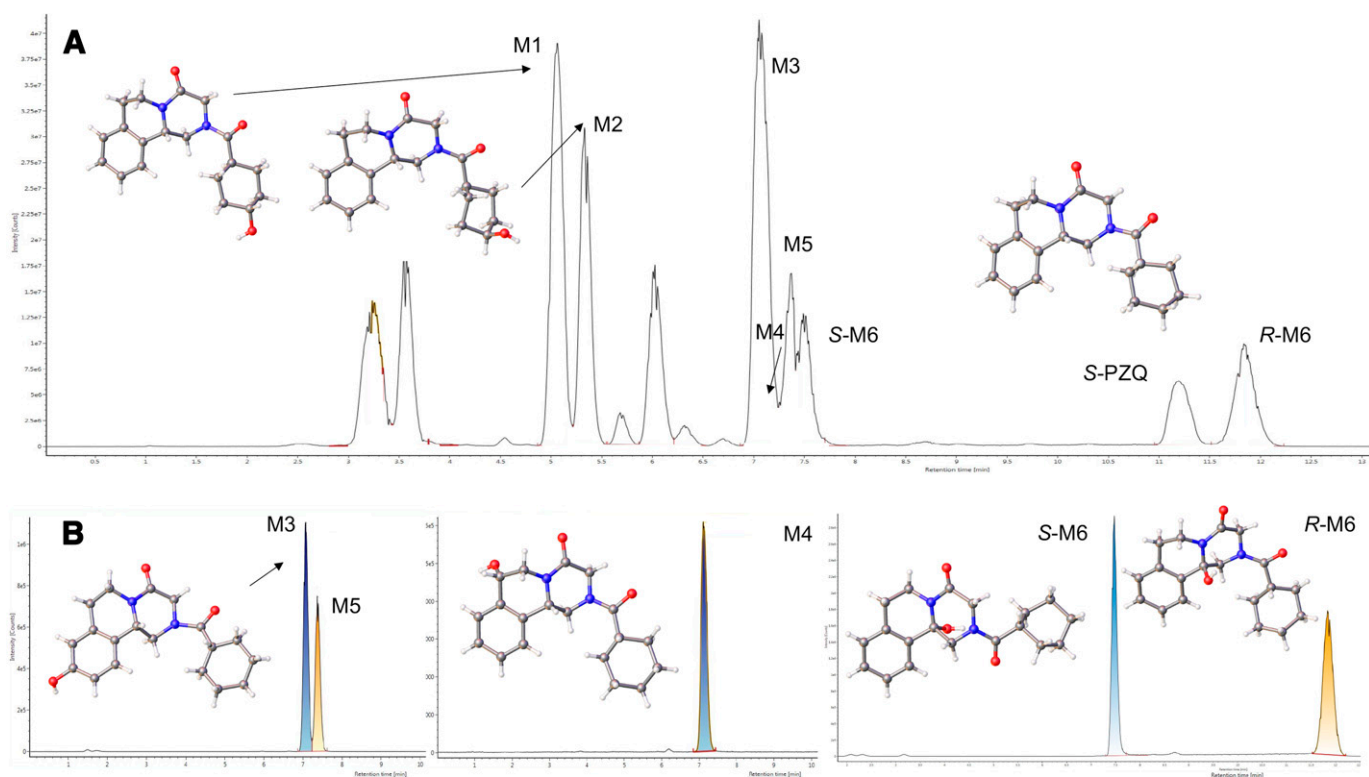


Fig. 3. Full-scan liquid chromatography mass spectrometry chromatograms of *S*-praziquantel (PZQ) incubated with human liver microsomes for 24 hours in the presence of nicotinamide adenine dinucleotide phosphate as cofactor on a Lux Cellulose-2 column (A) and PZQ metabolites M3–M6 after semi-preparative high-performance liquid chromatography separation and fractionation (B); M1, *S*-*trans*-4'-hydroxy-PZQ; M2, *S*-*cis*-4' hydroxy-PZQ, M3, *S*-9-hydroxy-PZQ; M4, *S*-7-hydroxy-*S*-PZQ; M5, still unknown; M6, *S*-11b-hydroxy-PZQ and *R*-11b-hydroxy-PZQ.

examined separately by CS-XRD. The soaking experiment of the first enantiomer of M6 showed the presence of one *S*-11b-hydroxy-PZQ molecule, but due to low occupancy of the analyte and therefore an insufficient chirality transfer from guest molecules to the host framework, the resulting inconclusive Flack value did not allow the confirmation of the chiral center. However, when analyzing the second enantiomer, one molecule of *R*-11b-hydroxy-PZQ (occupancy 100%) could be observed in the CS pores (R_1 7.32%; R_{int} 3.69%, $\chi =$

0.221(8)), hence indicating the identification of the first enantiomer to be in *S* configuration.

The refined crystallographic structures of *S*-PZQ and its hydroxy metabolites are shown in Fig. 3. Crystallographic data, ORTEP diagrams of the asymmetric unit including CS framework and analytes, reciprocal $h0l$ layers and Flack parameters before and after using solvent masking are shown in the Supplemental Data (Supplemental Fig. 1–22).

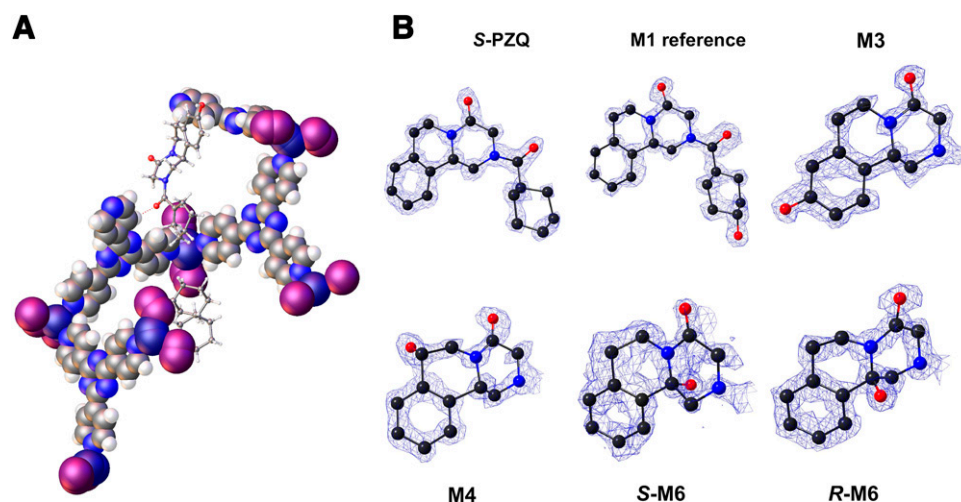


Fig. 4. (A) Asymmetric unit of $[(ZnI_2)_3(tpf)_2]_n$ with one *S*-9-hydroxy praziquantel (M3) and two cyclohexane molecules. The crystal structure exhibits C-H...O (red dashed line) interactions between the hydroxy metabolite and the crystalline sponge framework. (B) Electron density map F_o [contoured at 2.02σ (*S*-praziquantel), 2.00σ (M1 reference), 2.61σ (M3), 1.94σ (M4), 1.89σ (*S*-M6), 2.54σ (*R*-M6)] of the complete molecule of *S*-praziquantel and M1, as well as the core moiety of the incubation samples M3, M4, *S*-M6 and *R*-M6.

structure of the metabolite as a guest molecule in the CS pores, but MS and UV-VIS data strongly indicated that the hydroxylation occurred at the aromatic benzene ring. The structure of metabolite M6, which is known from literature, was confirmed, and the presence of both enantiomers *in vitro* was shown. The analysis of both enantiomers as a racemic mixture and individually after chiral separation allowed the determination of the respective configuration as *S*-11b-hydroxy-PZQ and *R*-11b-hydroxy-PZQ.

The application of CS-XRD for *S*-PZQ and its metabolites demonstrates that this technology can be applied for metabolite identification studies in drug discovery in which metabolites are only available in trace amounts from *in vitro* incubation. In comparison with the CS analysis, a high amount of substance was needed to conduct the NMR spectrum of M3, prolonging the lengthy sample purification process from days to weeks to collect sufficient analyte material. Furthermore, no information of the absolute configuration was obtained. The low abundance of metabolite M4 in the incubation solution only allowed the chromatographic preparation of 1–2 µg of sample material, which is insufficient for complete structure analysis by NMR. However, the CS-XRD could be applied and allowed the successful determination of M4.

Our results show that CS-XRD in combination with MS data are a valuable tool for absolute structure identification of metabolites in early phases of drug discovery and development, it constitutes a powerful tool for human metabolite identification from *in vitro* incubations and allows earlier risk mitigations associated with metabolites in safety testing guidelines (FDA, 2016). The technology was able to provide new knowledge of the metabolism of PZQ, which has been used for the treatment of schistosomiasis for decades. The structural information at the atomic level were gained using only trace amounts of analyte material, outlining a significant advantage in comparison with other techniques like MS or NMR. Thus, we successfully confirmed the structure of three known hydroxy metabolites and elucidated the complete molecular scaffold of two unknown metabolites of *S*-PZQ.

To fully benefit from this technology, further investigation of the CS method is still needed to expand the chemical space of possible guest analytes by applying new types of CS with different binding sites and pore sizes to successfully encapsulate a wide range of target analytes in the CS pores and thus to successfully elucidate their complete structure.

Acknowledgments

The authors gratefully thank Ralf-Erwin Licht for his excellent experimental contribution on metabolite profiling. We also acknowledge Holger Scheible, Dominique Perrin, Hanno Schieferstein and Benedikt Lang for useful discussions and support of this study.

Authorship Contributions

Participated in research design: Rosenberger, Badolo.

Conducted experiments: Rosenberger.

Contributed new reagents or analytic tools: Kühn, Georgi.

Performed data analysis: Rosenberger, Jenniches, Marx.

Wrote or contributed to the writing of the manuscript: Rosenberger, Jenniches, von Essen, Khutia, Kühn, Marx, Hirsch, Hartmann, Badolo.

References

- Biradha K and Fujita M (2002) A springlike 3D-coordination network that shrinks or swells in a crystal-to-crystal manner upon guest removal or readsorption. *Angew Chem Int Ed Engl* **41**:3392–3395.
- Brunet G, Safin DA, Aghaji MZ, Robeyns K, Korobkov I, Woo TK, and Murugesu M (2017) Stepwise crystallographic visualization of dynamic guest binding in a nanoporous framework. *Chem Sci (Camb)* **8**:3171–3177.
- Dolomanov OV, Bourhis LJ, Gildea RJ, Howard JAK, and Puschmann H (2009) OLEX2: a complete structure solution, refinement and analysis program. *J Appl Cryst* **42**:339–341 International Union of Crystallography.
- FDA (2016) *Safety Testing of Drug Metabolites - Guidance for Industry*, US Department of Health and Human Services FDA Center for Drug Evaluation and Research, Silver Spring, MD.
- Holcápek M, Jirásko R, and Lisa M (2010) Basic rules for the interpretation of atmospheric pressure ionization mass spectra of small molecules. *J Chromatogr A* **1217**:3908–3921.
- Hoshino M, Khutia A, Xing H, Inokuma Y, and Fujita M (2016) The crystalline sponge method updated. *IUCrJ* **3**:139–151.
- Huang J, Bathena SPR, and Alnouti Y (2010) Metabolite profiling of praziquantel and its analogs during the analysis of *in vitro* metabolic stability using information-dependent acquisition on a hybrid triple quadrupole linear ion trap mass spectrometer. *Drug Metab Pharmacokinet* **25**:487–499.
- Hübschle CB, Sheldrick GM, and Ditttrich B (2011) ShelXle: a Qt graphical user interface for SHELXL. *J Appl Cryst* **44**:1281–1284.
- Inokuma Y, Ukegawa T, Hoshino M, and Fujita M (2016) Structure determination of microbial metabolites by the crystalline sponge method. *Chem Sci (Camb)* **7**:3910–3913.
- Inokuma Y, Yoshioka S, Ariyoshi J, Arai T, Hitora Y, Takada K, Matsunaga S, Rissanen K, and Fujita M (2013) X-ray analysis on the nanogram to microgram scale using porous complexes [published correction appears in *Nature* (2013) 501:262]. *Nature* **495**:461–466.
- Kováč J, Vargas M, and Keiser J (2017) *In vitro* and *in vivo* activity of *R*- and *S*- praziquantel enantiomers and the main human metabolite trans-4-hydroxy-praziquantel against *Schistosoma haematobium*. *Parasit Vectors* **10**:365.
- Lerch C and Blaschke G (1998) Investigation of the stereoselective metabolism of praziquantel after incubation with rat liver microsomes by capillary electrophoresis and liquid chromatography-mass spectrometry. *J Chromatogr B Biomed Sci Appl* **708**:267–275.
- Meister I, Ingram-Sieber K, Cowan N, Todd M, Robertson MN, Meli C, Patra M, Gasser G, and Keiser J (2014) Activity of praziquantel enantiomers and main metabolites against *Schistosoma mansoni*. *Antimicrob Agents Chemother* **58**:5466–5472.
- Nieya L, Thelingwani R, Li XQ, Cavallin E, Isin E, Nhachi C, and Masimirembwa C (2019) The effect of ketoconazole on praziquantel pharmacokinetics and the role of CYP3A4 in the formation of X-OH-praziquantel and not 4-OH-praziquantel. *Eur J Clin Pharmacol* **75**:1077–1087.
- Park SK, Friedrich L, Yahya NA, Rohr CM, Chulkov EG, Maillard D, Rippmann F, Spangenberg T, and Marchant JS (2021) Mechanism of praziquantel action at a parasitic flatworm ion channel. *Sci Transl Med* **13**:eabj5832.
- Ramadhar TR, Zheng SL, Chen YS, and Clardy J (2015) Analysis of rapidly synthesized guest-filled porous complexes with synchrotron radiation: practical guidelines for the crystalline sponge method. *Acta Crystallogr A Found Adv* **71**:46–58.
- Ramanathan R, Su AD, Alvarez N, Blumenkrantz N, Chowdhury SK, Alton K, and Patrick J (2000) Liquid chromatography/mass spectrometry methods for distinguishing N-oxides from hydroxylated compounds. *Anal Chem* **72**:1352–1359.
- Rosenberger L, von Essen C, Khutia A, Kühn C, Georgi K, Hirsch AKH, Hartmann RW, and Badolo L (2021) Crystalline sponge affinity screening: A fast tool for soaking condition optimization without the need of X-ray diffraction analysis. *Eur J Pharm Sci* **164**:105884.
- Rosenberger L, von Essen C, Khutia A, Kühn C, Urbahns K, Georgi K, Hartmann RW, and Badolo L (2020) Crystalline Sponges as a Sensitive and Fast Method for Metabolite Identification: Application to Gemfibrozil and Its Phase I and II Metabolites. *Drug Metab Dispos* **48**:587–593.
- Sakurai F, Khutia A, Kikuchi T, and Fujita M (2017) X-ray Structure Analysis of N-Containing Nucleophilic Compounds by the Crystalline Sponge Method. *Chemistry* **23**:15035–15040.
- Schepmann D and Blaschke G (2001) Isolation and identification of 8-hydroxypraziquantel as a metabolite of the antischistosomal drug praziquantel. *J Pharm Biomed Anal* **26**:791–799.
- Sheldrick GM (2015) Crystal structure refinement with SHELXL. *Acta Crystallogr C Struct Chem* **71**:3–8.
- Vendrell-Navarro G, Scheible H, Lignet F, Burt H, Luepfert C, Marx A, Abla N, Swart P, and Perrin D (2020) Insights into Praziquantel Metabolism and Potential Enantiomeric Cytochrome P450-Mediated Drug-Drug Interaction. *Drug Metab Dispos* **48**:481–490.
- Wang H, Fang ZZ, Zheng Y, Zhou K, Hu C, Krausz KW, Sun D, Idle JR, and Gonzalez FJ (2014) Metabolic profiling of praziquantel enantiomers. *Biochem Pharmacol* **90**:166–178.
- World Health Organization (2011) Schistosomiasis: number of people treated in 2009. *Wkly Epidemiol Rec* **86**:73–80.
- World Health Organization (2020) Schistosomiasis fact sheet. <https://www.who.int/news-room/fact-sheets/detail/schistosomiasis>.

Address correspondence to: Lara Rosenberger, Frankfurter Strasse 250, 64293 Darmstadt, Germany. E-mail: Lara.Rosenberger@emdgroup.com